HEDL-SA-202

CONF-710622--2

COMPUTER SIMULATION OF THE SHORT-TERM ANNEALING OF DISPLACEMENT CASCADES

By

D. G. Doran
WADCO Corporation
Richland, Washington

and

R. A. Burnett
Battelle-Northwest
Richland, Washington

April 1971

Hanford Engineering Development Laboratory, Richland, Washington, operated by WADCO Corporation, a subsidiary of Westinghouse Electric Corporation for the United States Atomic Energy Commission under Contract No. AT(45-1)-2170

This paper covers work performed by Battelle-Northwest under AEC Contract No. AT(45-1)-1830 and WADCO Corporation under AEC Contract No. AT(45-1)-2170. To be presented at the Battelle Material Sciences Colloquium in Seattle, Washington, and Harrison Hot Springs, B.C., Canada, on June 14-19, 1971.

COMPUTER SIMULATION OF THE SHORT-TERM ANNEALING OF DISPLACEMENT CASCADES

by

D. G. Doran
WADCO Corporation
Richland, Washington

and

R. A. Burnett
Battelle-Northwest
Richland, Washington

ABSTRACT

An important source of damage to a solid exposed to high energy neutrons (or ions) is the displacement of atoms from normal lattice sites. In a fast reactor, energies of tens of keV may be transferred to an atom and thus initiate a displacement cascade consisting of a localized high density of interstitials and vacancies. These defects will subsequently interact with one another to form clusters and to reduce their density by mutual annihilation. This short-term annealing has been simulated with a small computer using an atomic model of γ-iron based on the work of Johnson. The input cascades are due to Beeler. Results were obtained with both large (104 sites) and small (32 sites) annihilation regions. The former results in about one-half the residual defects of the latter, and a smaller fraction of clustered defects. Cluster size distributions and several examples of spatial distributions are given. It is shown that the principal effect of randomizing the spatial distribution of defects in a typical cascade geometry is to diminish vacancy clustering and enhance interstitial clustering.

1 INTRODUCTION

An important source of damage to a solid exposed to high energy neutrons (or ions) is the displacement of atoms from normal lattice sites. In a fast reactor, energies of tens of keV may be transferred to the primary knock-on atom (PKA), producing in medium and high atomic weight materials a displacement cascade comprising a localized high density of vacancies and interstitials. These defects will subsequently interact with one another to produce clusters and to reduce their density by mutual annihilation--a process called short-term annealing in the present context.

The objective of this work was to determine by computer simulation the defect clustering characteristics of γ-iron, a stand-in for the stainless steel used in fast reactors. Both high and low temperatures were studied, but only the high temperature results will be reported here. Also investigated was the influence of the cascade formation process on the short-term annealing characteristics of a given density of defects. This was examined with a "randomized cascade" created by introducing defects at randomly selected positions within a typical cascade volume.

In a previous paper[1] the annealing simulation work initiated by Beeler and Besco[2,3] was extended and applied to a description of short-term annealing of cascades in α-iron (bcc lattice). This paper is concerned with a new program to simulate short-term annealing in an fcc lattice, and its application to cascades produced by Beeler.[2] The new code employs a model for γ-iron based on the work of R. A. Johnson.[4] Beeler used a copper model in his fcc work, but there is

no basis for distinguishing between copper and γ-iron at the present level of sophistication.

2 COMPUTATIONAL DETAILS

2.1 The Machine

A hybrid computer facility* consisting of a Beckman 2133 analog computer and a PDP-7 digital computer (8K memory) was used in this work. Actually, a random noise generator used to generate random numbers was the only contribution from the analog side. The digital program, HAPFCC (Hybrid Anneal Program--FCC), was written in assembly language.

The primary reason for using the small computer is the high level of man-machine interaction it provides--a significant consideration because the annealing runs are open-ended. Parameters can be changed through teletype entry at the beginning of a run, and several options can be exercised through console switches to control a run in progress. In addition, the program runs faster than an equivalent FORTRAN program on the available big machine (a UNIVAC 1108) and the charge rate is much lower on the small machine.

Initial defect distributions were read into the computer from punched cards, and intermediate and final distributions were stored on magnetic tape. Both tabular and graphic outputs were recorded with an electrostatic line printer.

HAPFCC can handle a maximum of 432 defect pairs within that portion of the 8K memory not required for program instructions. This was sufficient to handle the largest cascades presently available but was a

---

* Operated by Computers and Control Section of Battelle-Northwest.

minor limitation in studying randomized cascades, as will be apparent below.

2.2 Program Description and Operation

The annealing program, a correlated random walk on an fcc lattice, is defined by the following: the identity of mobile defects, jump vectors and jump probabilities of mobile defects, definition of correlated jumps and their relative jump probabilities, clustering criteria, and annihilation criteria.

During each time step, each member of each migrating cluster (of the appropriate type) is considered once, in random order, for a jump. A permissible jump vector is chosen at random, possible correlations sought, and the jump performed or not performed according to the assigned probability through selection of another random number. If a jump results, an examination is made for possible clustering or annihilation.

High temperature (nominally 800°K) operation was characterized by two successive stages because of the large difference in mobilities of vacancies and interstitials. During the high temperature-interstitial stage, the much slower vacancies were ignored except as they participated in annihilation of migrating interstitials. During the subsequent vacancy stage, interstitials were immobilized to conserve computer time. This procedure poses no problem at the beginning of the vacancy stage because only immobile interstitial complexes remain in the vicinity of the vacancies. Ultimately, however, some of the by-products of annihilation are mobile interstitials. An effort was made to determine the behavior of the newly created mobile interstitials (see Section 4).

The time step in the high temperature-interstitial stage was such that the uncorrelated jump probability of the most mobile defect (I_1)* was 0.5; the correlated probability was unity. The vacancy stage time step was chosen so that the highly mobile V_2 jumped once per step.**

It was found that 1000 to 2000 time steps in a given stage generally reduced the frequency of defect interactions to the order of one per 500 steps.

Ten 20 keV and ten 5 keV cascades were selected for processing. These cascades are a subset of those which provided the cluster size distributions of reference 2. Such distributions were obtained by Beeler from a computer program CLUSTER which applied clustering criteria to the output of the CASCADE program. For the present work, only the CASCADE outputs were utilized. Inherent in them is the recombination of all related interstitial-vacancy pairs (unrelated pairs are not recognized) separated by less than $\sqrt{5}$ half-lattice units; the interstitials are at octahedral sites. The initial operation of the HAPFCC program is to assign each octahedral interstitial to a randomly chosen neighboring fcc site and to assign to it an orientation along a randomly chosen major axis.

The spatial distribution of defects in a displacement cascade is a rather special one in which a vacancy-rich central region is surrounded by an interstitial-rich peripheral region. An effort was made to determine how strongly this configuration influences the cluster size distribution. The geometrical configuration of one 20 keV cascade

---

* The symbols I_n and V_n designate interstitial and vacancy clusters, respectively, of size n.

** The relative jump probabilities should be reasonably representative of the temperature range 600-1000°K.

(No. 2076) was determined by computer-plotting the defects plane by plane; a simplified representation of the contribution from each plane was used (see Figure 1). A library of alternating interstitial and vacancy sites was prepared by randomly selecting sites within the geometrical figure that resulted from stacking the slabs (total volume of $\sim$15,000 hlu^3).* A "randomized cascade" was created by selecting 400+ defects of each type from this library, eliminating unlike defects which were first or second neighbors (as was done with 20 keV cascades), adding more defects, etc., until the desired number of defects was reached. This iterative procedure was necessary because of the program limitation of 432 defect pairs. Only two iterations were required to reach the goal of $\sim$250 pairs, the number of defects in a 20 keV displacement cascade after first and second neighbor unlike defects have recombined.

3 THE γ-IRON MODEL

The model is based on Johnson's[4] simulation of point defects and small clusters in γ-iron. The activation energies found by him lead to the following hierarchy of the mobile defects included in this work, starting with the most mobile: I_1, I_2, I_3, V_2, V_3, V_4, and V_1. The large gap in mobility between the slowest moving interstitial (I_3) and the fastest moving vacancy (V_2), even at high temperatures, led to separate interstitial and vacancy annealing stages in HAPFCC.

Johnson found interstitial behavior to be very complex and his treatment is incomplete. Even so, we have not attempted to incorporate all of his results but have tried to retain their essence.

---

* hlu $\equiv$ half-lattice unit.

The stable I_1 is, following Johnson, the <100> split interstitial. In migrating, an x-oriented I_1 can jump to 8 possible first neighbor sites such that $\Delta x = \pm 1$; e.g., a jump in the x-z plane corresponds to $\Delta y = 0$, $\Delta z = \pm 1$ and a new (z) orientation. The motion of an I_1 that is within a 4th neighbor separation of another I_1 is correlated such that the jump probability is unity toward the formation of the stable I_2 (see Figure 2-a). If relative orientations preclude stable I_2 formation, the jump probability for increasing the separation is unity. If an I_1 is within a 4th neighbor separation of a clustered interstitial or two or more interstitials (clustered or single), a jump to decrease the total separation has a probability of unity, while a jump to increase the total separation is not permitted.

In addition, a longer ranged correlation for single interstitials can be used; viz., a jump toward another interstitial has probability α if the proposed jump site is a 4th or nearer neighbor of the other interstitial (in the present work, $\alpha = 1$).

A first neighbor bond constitutes clustering. The I_2 configuration is always two parallel interstitials, their common orientation being perpendicular to a line joining their centers (see Figure 2-a). The I_2 migrates only in the plane perpendicular to its orientation, with an uncorrelated jump probability of 0.12 relative to the I_1. The 4th neighbor correlation scheme above applies to each member of an I_2.

The I_3 is permitted to exist in two I_3 (112)* configurations (see Figure 2-b, c). Since the I_2 is already in the most stable configuration, the third interstitial can take up one of four sites in the plane

---

* Indicates 3 bonds, 2 of which are 1st neighbor bonds and one of which is a 2nd neighbor bond.

perpendicular to the orientation of the I_2. Furthermore, it can be oriented parallel to the I_2 or lie in the plane of the I_3; the latter (Figure 2-b) was found by Johnson to be the lowest energy configuration. Migration of the "parallel" I_3 is confined to the plane of the defect, but the most stable I_3 can migrate in three dimensions. Jump probabilities relative to the I_1 are 0.011, but the stable form can reorient with a relative probability of 1.0.

An interstitial cluster of size 4 or larger is considered immobile and no orientation information of its members is retained. Hence the morphology of the cluster has no significance. No dissociation of clusters is permitted.

Mobile species of vacancies are confined to V_1, V_2, V_3, and V_4. Either member of the V_2, a nearest neighbor pair, can jump to one of the 4 first neighbor sites in the plane bisecting their bond. Dissociation of the V_2, or any vacancy cluster, is not permitted.

The stable forms of the V_3 and V_4 are the triangle, $V_3(111)$, and the tetrahedron, V_4 (111111), and these configurations are immediately imposed when such clusters form. The V_3 can reorient by shifting the associated vacancy among the 4 sites of the tetrahedron; the reorientation frequency is equivalent to the V_2 jump frequency. The V_3 migrates with either a V_3 (112) or V_3 (113) intermediate state. The V_4 migrates effectively one half-lattice unit in a <100> direction, undergoing simultaneously a 90° rotation. Higher order vacancy clusters are considered immobile.

Vacancy correlations, limited to short range, are summarized in Table 1. Some of the associated activation energies are based on work by the authors using Johnson's γ-iron potential in the code

DEFECT.* Relative jump probabilities are, of course, dependent on the temperature.

An important but inadequately defined parameter, the annihilation region (AR), describes the attraction of a vacancy for an interstitial and the resulting annihilation of both defects. The AR is a set of sites relative to the position of the interstitial and dependent on its orientation, such that, if a vacancy occupies one of the sites, the interstitial and vacancy are considered to suffer mutual annihilation.

In a previous paper,[1] the AR was taken to increase with temperature, but this procedure was probably unjustified.[5] For temperatures so low that interstitial migration is rare, the effective AR would indeed increase with temperature, but as interstitials become freely migrating the vacancy sinks will lose their effectiveness and the effective AR will decrease.

The approach in the present work is to study the sensitivity of the results to the AR by using two regions (see Table 2). The small AR is the 32 site spontaneous (0°K) annihilation region determined by Johnson; the large AR is a 104 site region obtained by moving one interstitial jump beyond the 32 site region.

4 RESULTS AND DISCUSSION

4.1 Displacement Cascades

4.1.1 Time History. As indicated above, computer runs were continued until defect interactions became infrequent--generally 1000 to 2000 time steps in each stage. One cascade was carried to 4000 time

---

* The principal difference between DEFECT, developed by Beeler, and Johnson's program is that a rigid boundary in the former replaces the elastic continuum of the latter.

steps; in this case, no interactions occurred after 2000 steps.

Little annihilation took place in the vacancy stage relative to that in the interstitial stage, but there was a general increase in the fraction of mobile interstitials. This occurs when a migrating vacancy interacts with an immobile interstitial cluster so as to reduce the cluster (or a portion of it) to size 3 or less. (Of course, there is general attrition of larger clusters also.) Several runs in which this phenomenon was prominent were continued in the interstitial mode to discover the fate of the newly created mobile defects. It was found that there is a strong tendency for these newly created defects to re-cluster with one another.

Decreasing the AR from 104 to 32 sites simply increased the rate of annihilation by the same factor that the defect population was increased; i.e., the percentage decrease per time step in the number of defects was the same in both cases.

4.1.2 Residual Annihilation and Clustering. The mutual annihilation of interstitials and vacancies that occurred during the short-term annealing simulation is summarized in Table 3. The number of residual defects was approximately 2 pair/keV between 5 and 20 keV for the large AR and $\sim$4 pair/keV for the small AR. The cluster size distributions are given in Tables 4 and 5. With the large AR, 20-30%* of the surviving interstitials and 40-60% of the surviving vacancies are clustered. Most of the other defects migrate away and lose their identification with the cascade. The corresponding numbers for the small AR are 35-50% of the surviving interstitials and 60-70% of the surviving vacancies.

---

* The percentage varied with cascade energy. In each case, the first number corresponds to 5 keV, the second to 20 keV.

The spatial distribution of defects is illustrated in Figures 3 to 5. In each post-anneal configuration, the mobile interstitials have been removed in order to account for the 10^6-10^8 jumps that each would have made, if permitted, during the vacancy stage. The quasi-channeled cascade of Figure 4 (in which no immobile interstitial clusters survived) was the only one of its type studied. More common was the rather compact cascade shown in Figure 5 which served as the model for the randomized cascade. In regard to 5 keV cascades, it was not uncommon to have no residual immobile interstitial clusters (i.e., $I_{\geq 4}$) or vacancy clusters ($V_{\geq 5}$) when the large AR was used.

4.1.3 Effect of Annihilation Region. Results for large and small ARs are directly compared for 20 keV cascades in Figure 6. Plotted are the fractional distributions of residual defects (i.e., each sums to unity) in clusters to show the influence of the AR on the relative clustering within a cascade. An absolute comparison is easily made using Tables 3 to 5. The small AR promoted clustering of both interstitials and vacancies. The results for 5 keV cascades were similar, but shifted somewhat toward smaller cluster sizes.

4.1.4 Energy Dependence. Fractional defect distributions for 20 and 5 keV cascades are compared in Tables 4 and 5. At 5 keV, there are relatively more single interstitials and fewer large clusters. Maximum interstitial cluster sizes were 8 and 5 for 20 and 5 keV, respectively, for the large AR and 10 and 8, respectively, for the small AR. The number of interstitial clusters generally increased faster than the energy for the two energy values investigated; e.g., the number of clusters of size ≥ 4 was proportional to $E^{1.2}$.

In the case of vacancies, 5 keV cascades had proportionately more

small clusters than 20 keV cascades and also proportionately more large clusters. The latter was especially true for the large AR, for which the maximum cluster size was 11 at each energy. The small AR resulted in maximum cluster sizes of 22 and 12 for 20 and 5 keV cascades, respectively.

The number of vacancy clusters generally increased faster than the energy, as for interstitials. For clusters of size ≥ 4 (or ≥ 5) the number per cascade was proportional to $E^{1.3}$.

4.2 Randomized Cascades

4.2.1 Time History. Two randomized cascades, patterned after the same displacement cascade but with independent defect configurations, were run in high temperature simulations with both large and small AR. The rate of annihilation was the same as for the corresponding displacement cascade runs. The decrease in the fraction of mobile interstitials with time during the interstitial stage, however, was surprisingly insensitive to the value of the AR, and the rate of decrease was higher than the average rate exhibited by the real displacement cascades for either value of the AR.

4.2.2 Residual Annihilation and Clustering. The results of mutual annihilation for the randomized cascades is summarized in Table 6. The small AR resulted in 70% more residual defects than the large AR.

Clustering of defects in randomized cascades is summarized in Table 7. The creation of mobile interstitials in the vacancy stage was common in these runs, particularly for the small AR case; hence the distributions are weighted somewhat toward small cluster sizes.

Cluster size distributions for randomized cascades and actual cascades are compared in Figures 7 and 8. There is a significant

difference in sensitivity to the AR in the two cases. The randomized cascades were sensitive only at the large cluster end of the distributions for both interstitials and vacancies. The maximum interstitial cluster size was decreased somewhat while the maximum vacancy cluster size was increased by decreasing the AR. Actual cascades, on the other hand, exhibited a decrease in small clusters and an increase in large clusters when the AR was decreased. It is this difference in behavior that gives rise to the AR effect that is apparent in Figures 7 and 8.

The decreased influence of a change in the AR on the randomized cascades is probably a result of the more uniform spatial distribution of defects in this case. It appears that the mean distance between interstitials is significantly increased and hence clustering decreased by increasing the AR in the case of actual cascades, but not for randomized cascades. The same is true for vacancies, but the bunching of vacancies in actual cascades (as, for example, in Figure 1) causes enhanced vacancy clustering for either AR relative to the randomized cascades.

The spatial distribution of defects in one of the randomized cascades is shown in Figure 9 for direct comparison with Figure 5. The difference in interstitial clustering is particularly evident.

4.3 Comparison With α-Iron (bcc)

In previous work[1] on short-term annealing, a model of α-iron (bcc) was used in which a 62 site AR was employed for high temperature runs and a 30 site AR for low temperature runs.

The annihilation characteristics of the α-iron data are included in Table 3 for comparison with the present results. It would, of course, be expected that present results obtained with the large AR would be

most comparable to the α-iron results. In fact, the effective difference between the 62 site bcc region and the 104 site fcc region is less than suggested by the number of sites involved. The bcc annihilation region is very anisotropic, extending farthest along the close-packed directions (<111>), whereas the fcc annihilation region is more nearly isotropic. Unpublished work by the authors has shown that, in the bcc case, an isotropic region encompassing 112 sites produces annihilation approximately equivalent to the 62 site region.

The similarity in the high temperature results, after the initial annihilation, is indeed striking and certainly somewhat coincidental* considering the numerous differences in the manner in which runs were made in the two cases.

Some of the results on the cluster size distributions for α-iron are included in Tables 3 to 5. The large AR γ-iron results are quite similar to the α-iron results for both interstitials and vacancies. The major difference is the lower production of large vacancy clusters ($\geq$10) by 20 keV cascades in the fcc case.

5 SUMMARY AND CONCLUSIONS

The displacement cascades simulated by Beeler[2] have been "temperature corrected" (to nominally 800°K) by means of a simulated short-term anneal. The annealing model was based on the simulation of γ-iron by Johnson.[4] Results were obtained with both large (104 sites) and small (32 sites) annihilation regions; the latter is considered the more realistic at the nominal temperature.

It was found that the 104 site annihilation region led to the

---

* Low temperature runs were less similar.

survival of ∿2 Frenkel pairs/keV between 5 and 20 keV; the 32 site region led to ∿4 Frenkel pairs/keV. With the large annihilation region, 20-30% of the surviving interstitials and 40-60% of the surviving vacancies are clustered--the other defects migrate away and lose their identification with the cascade. The corresponding numbers for the small annihilation region are 35-50% of interstitials and 60-70% of vacancies. The number of clusters per cascade increased somewhat faster than the energy.

The principal effects of randomizing the spatial distribution of defects in a typical cascade geometry were to diminish vacancy clustering and enhance interstitial clustering somewhat.

REFERENCES

1. Doran, D. G.: Rad. Effects, 2: 249 (1970).
2. Beeler, Jr., J. R.: Phys. Rev., 150: 470 (1966).
3. Besco, D. G.: General Electric Company Tech. Report GEMP-644, 1967.
4. Johnson, R. A.: Phys. Rev., 145: 423, 152: 629 (1966).
5. Merkle, K. L.: Private Communication.

FIGURE CAPTIONS

1. A single plane through the pre-anneal configuration of a 20 keV cascade (No. 2076), and its representation used in defining a randomized cascade.
2. Interstitial configurations studied by Johnson.[4] (a) The stable I_2. (b) The most stable I_3. (c) An alternative form of I_3.
3. A projection on to two planes of a 5 keV cascade. Squares and Xs are vacancies and interstitials, respectively. Take off point of PKA is 200, 200, 200; direction is shown by arrow. Dimension is half-lattice constant. (a) Pre-anneal. (b) High temperature post-anneal, 32 site AR. (c) High temperature post-anneal, 104 site AR.
4. A quasi-channeled 20 keV cascade (No. 2079). See caption Figure 3. (a) Pre-anneal. (b) High temperature post-anneal, 104 site AR.
5. A compact 20 keV cascade (No. 2076). See caption Figure 3. (a) Pre-anneal. (b) High temperature post-anneal, 32 site AR. (c) High temperature post-anneal, 104 site AR.
6. A comparison of the distribution of defects in clusters after simulated high temperature anneals using small and large annihilation regions.
7. A comparison of integral distributions of interstitials in clusters for displacement cascades and "randomized cascades."
8. A comparison of integral distributions of vacancies in clusters for displacement cascades and "randomized cascades."
9. A "randomized cascade" (No. 77). See caption Figure 3. (a) Pre-anneal. (b) High temperature post-anneal, 32 site AR. (c) High temperature post-anneal, 104 site AR.

Table 1. Vacancy Correlations

Defect	Jump Type	Activation Energy (ev)	Jump Probability Relative to Isolated V_2
V_1	Isolated jump	1.32	0.002
V_1[a]	One 2→1[b]	1.28	0.004
	Two 2→1	1.24	0.007
	One 3→1	1.07	0.086
	One 4→1	1.07	0.086
	Two 3→1	0.82	1.0
	Two 3→1 + One 4→1	0.57	1.0
	Four 3→1	0.32	1.0
V_2[c]	Isolated jump	0.9	1.0
V_3[c]	Reorientation	0.9	1.0
	Isolated jump	1.02	0.165
V_4[c]	Isolated jump	1.15	0.024

[a] May be single or member of a cluster.

[b] m→n designates jump from m^{th} neighbor separation to n^{th} neighbor separation.

[c] Data refer to one member of the cluster.

Table 2. Annihilation Regions

Let split interstitial be located at origin and oriented in direction b.

Neighbor	Type	Exceptions	Number
	Small Region (32 sites)		
1	110	$\Delta b = 0$	8
3	211	$\Delta b = \pm 2$	16
4	220	$\Delta b = 0$	8
	Large Region (104 sites)		
1	110	$\Delta b = 0$	8
2	200	$\Delta b \neq 0$	4
3	211	$\Delta b = \pm 2$	16
4	220	none	12
5	310	$\Delta b = 0$	16
6	222	none	8
7	321	$\Delta b = \pm 2$	32
9	330	$\Delta b = 0$	8

Table 3. Average Annihilation Characteristics

Annealing Stage	Number of Defect Pairs					
	γ-Iron (Present Work)				α-Iron (Ref. 1)	
	20 keV		5 keV		20 keV	5 keV
	Large AR[a]	Small AR[b]	Large AR[a]	Small AR[b]	(c)	(c)
CASCADE output	406	406	93	93		
CASCADE output, 1st and 2nd neighbors annihilated	253	253	---	---		
	High Temperature					
After initial annihilation	107	188	25	50	140	40
After interstitial stage	52[d]	102[d]	12[d]	22[e]	50	13
After vacancy stage	43[f]	79[f]	11[f]	19[g]	42	12

[a] 104 site AR.

[b] 32 site AR.

[c] 62 site AR.

[d] 2000 steps in interstitial stage.

[e] 1000 steps in interstitial stage.

[f] Additional 2000 steps in vacancy stage.

[g] Additional 1000 steps in vacancy stage.

Table 4. Interstitial Cluster Size Distributions, High Temperature Case

n	Number of Interstitial Clusters of Size n per Cascade					
	γ-Iron					
	20 keV		5 keV		α-Iron (Ref. 1)	
	Large AR[a]	Small AR[b]	Large AR[a]	Small AR[c]	20 keV	5 keV
1	11.7	12.5	6.0	5.9		
2	5.9	5.0	1.0	1.5		
3	2.6	6.25	0.3	1.2		
4	1.7	3.0	0.3	1.2		
5	0.3	2.5	0.2	0.1		
6	0.4	1.5	0	0		
7	0.1	1.0	0	0.1		
8	0.1	0	0	0.1		
9	0	0	0	0		
10	0	0.25	0	0		
≥ 3	5.2	14.5	0.8	2.7	6.6	1.9
≥ 4	2.6	8.25	0.5	1.5	2.5	0.4
≥ 5	0.9	5.25	0.2	0.3	0.8	0

[a]Average of 10 cascades; 2000 interstitial + 2000 vacancy time steps.
[b]Average of 4 cascades; 1000 interstitial + 1000 vacancy time steps.
[c]Average of 10 cascades; 1000 interstitial + 1000 vacancy time steps.

Table 5. Vacancy Cluster Size Distributions, High Temperature Case

n	Number of Vacancy Clusters of Size n per Cascade					
	γ-Iron					
	20 keV		5 keV		α-Iron (Ref. 1)	
	Large AR[a]	Small AR[b]	Large AR[a]	Small AR[a]	20 keV	5 keV
1	10.2	15.2	3.8	4.8		
2	1.2	1.75	0.6	0.8		
3	0.6	0.25	0.3	0.4		
4	0.6	1.0	0.1	0.1		
5	1.3	1.5	0.2	0.3		
6	0.6	1.75	0	0.1		
7	0.9	0.5	0	0.2		
8	0.3	1.0	0.1	0.1		
9	0.4	0.5	0.1	0.1		
10	0.2	0.25	0.1	0		
>10	0.2[c]	1.75[d]	0.1[e]	0.5[f]		
$\geq$4	4.5	8.25	0.7	1.4	3.7	1.0
$\geq$7	2.0	4.0	0.4	0.9	1.8	0.5
$\geq$10	0.4	2.0	0.2	0.6	0.7	0.12

[a] Average of 10 cascades.

[b] Average of 4 cascades.

[c] $2V_{11}$ in 10 cascades.

[d] V_{11}, $3V_{12}$, V_{13}, V_{14}, V_{22} in 4 cascades.

[e] V_{11} in 10 cascades.

[f] $5V_{12}$ in 10 cascades.

Table 6. Average Annihilation Characteristics of Randomized Cascades, High Temperature

Annealing Stage	Number of Defect Pairs	
	Large AR	Small AR
Initial loading--1st and 2nd neighbor annihilation	257	257
After complete initial annihilation	118	186
After interstitial stage (1000 steps)	62	111
After vacancy stage (1000 steps)	54	91

Table 7. Cluster Size Distributions for Randomized Cascades, High Temperature

Number of Clusters of Size n per Randomized Cascade[a]					
Interstitials			Vacancies		
n	Large AR	Small AR	n	Large AR	Small AR
1	5.0	9.5	1	19.0	35.5
2	4.0	5.0	2	1.0	3.5
3	2.0	7.5	3	0	1.5
4	3.0	2.0	4	3.0	2.5
5	1.5	1.5	5	2.0	1.0
6	1.0	3.5	6	0	1.0
7	0	1.0	7	1.0	1.5
8	0.5	0	8	0.5	0
9	0	0	9		0
10	0	0.5	10		0
>10[b]	0.5		>10		1.0[c]
≥ 3	8.5	16.0	≥ 4	6.5	7.0
≥ 4	6.5	8.5	≥ 7	1.5	2.5
≥ 5	3.5	6.5	≥ 10	0	1.0

[a] Average of two "cascades"

[b] $1\text{-}I_{11}$ in two "cascades"

[c] $1\text{-}V_{11}$ and $1\text{-}V_{13}$ in two "cascades"

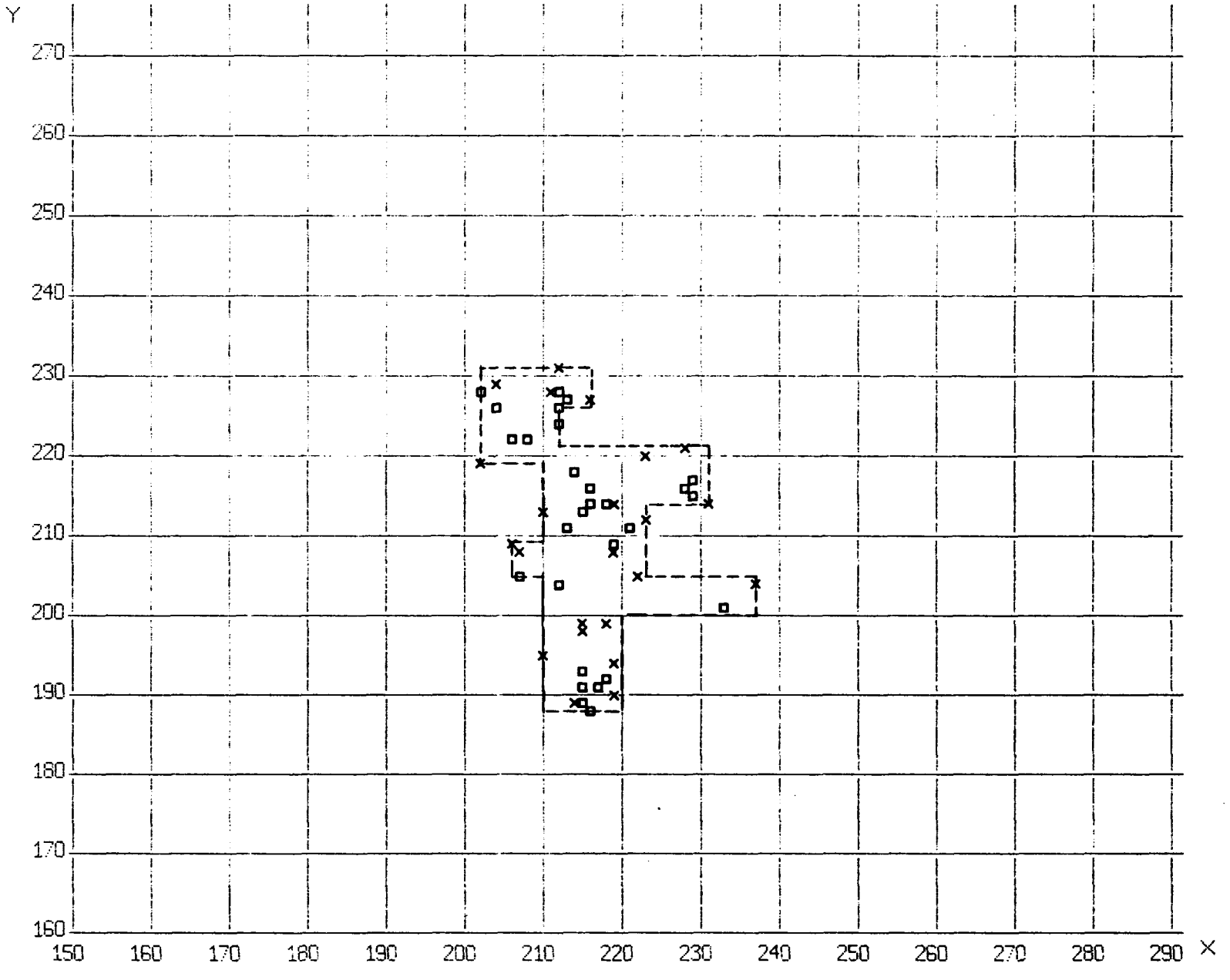
Y
270
260
250
240
230
220
210
200
190
180
170
160
150
160
170
180
190
200
210
220
230
240
250
260
270
280
290
X

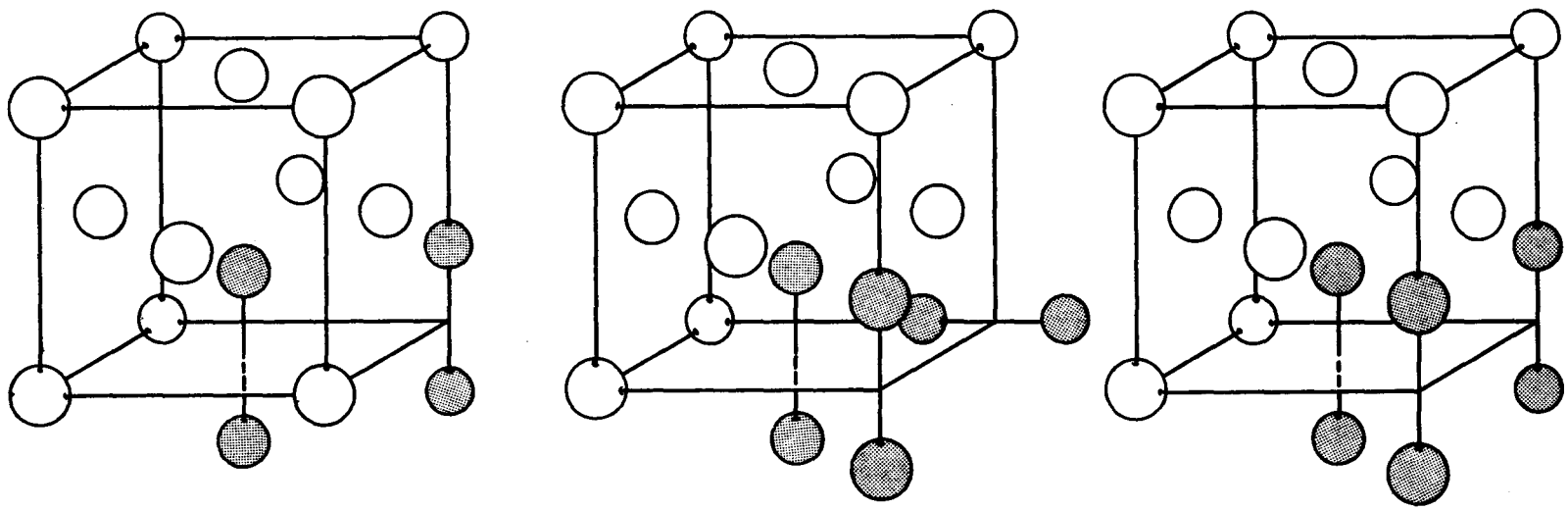
A
B
C

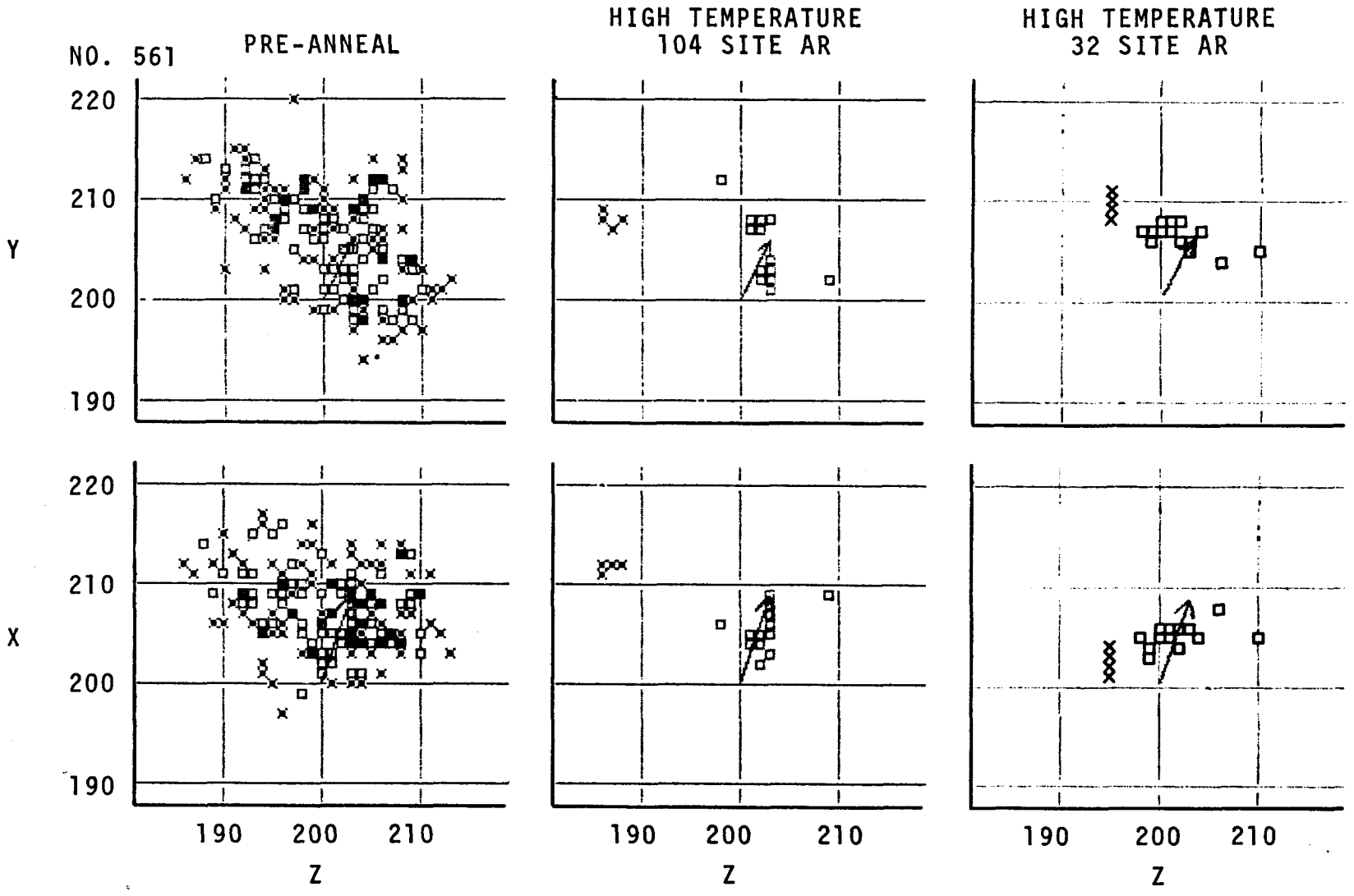
NO. 561
PRE-ANNEAL
HIGH TEMPERATURE
104 SITE AR
HIGH TEMPERATURE
32 SITE AR
Y
X
220
210
200
190
190
200
210
Z

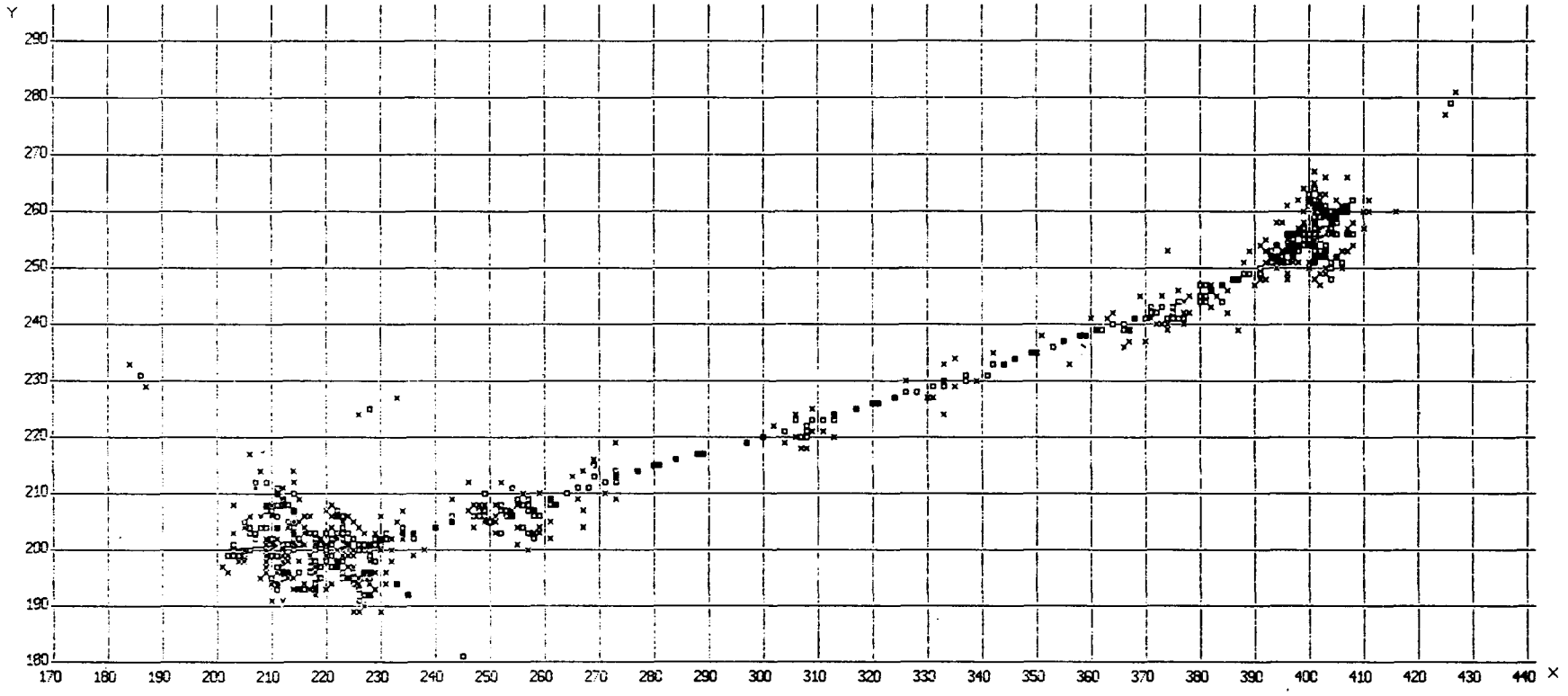
Y
290
280
270
260
250
240
230
220
210
200
190
180
170
180
190
200
210
220
230
240
250
260
270
280
290
300
310
320
330
340
350
360
370
380
390
400
410
420
430
440
X

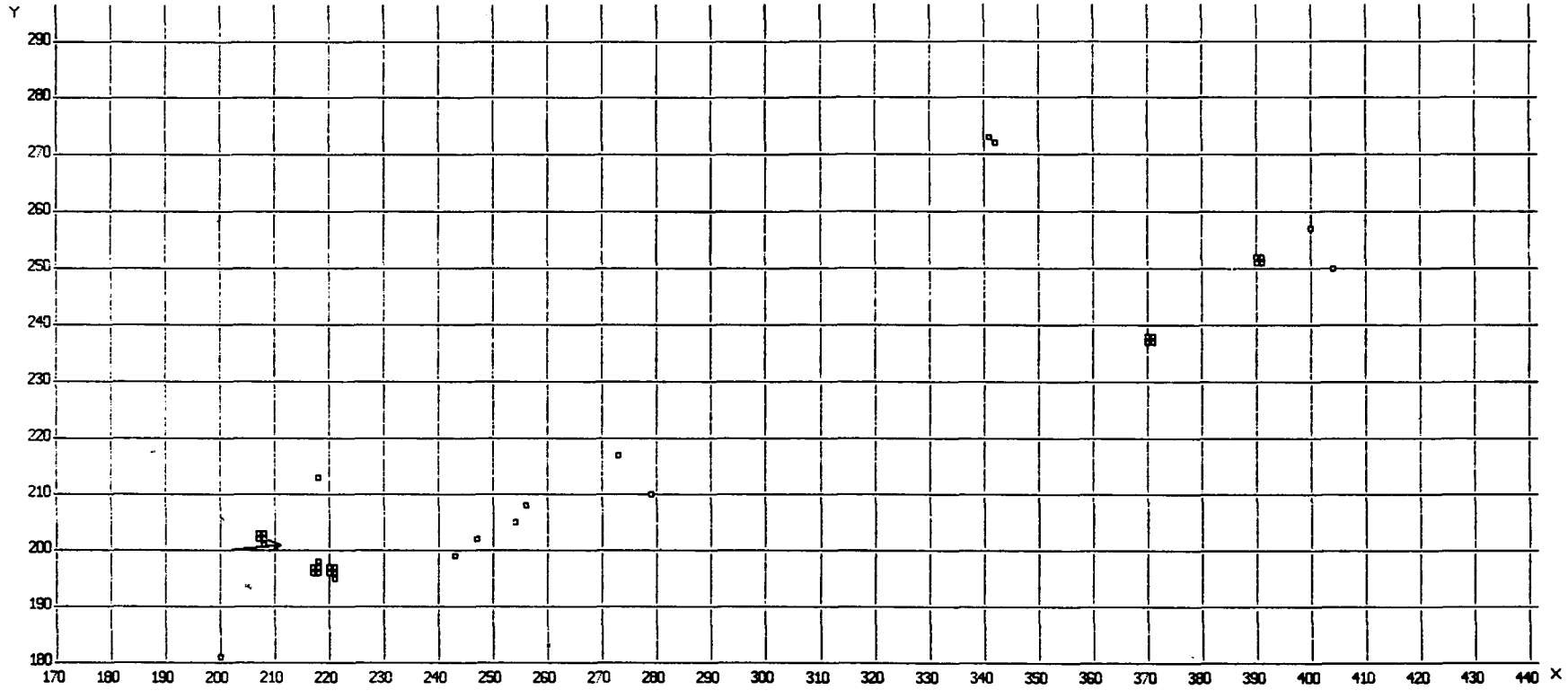
Y
290
280
270
260
250
240
230
220
210
200
190
180
170 180 190 200 210 220 230 240 250 260 270 280 290 300 310 320 330 340 350 360 370 380 390 400 410 420 430 440
X

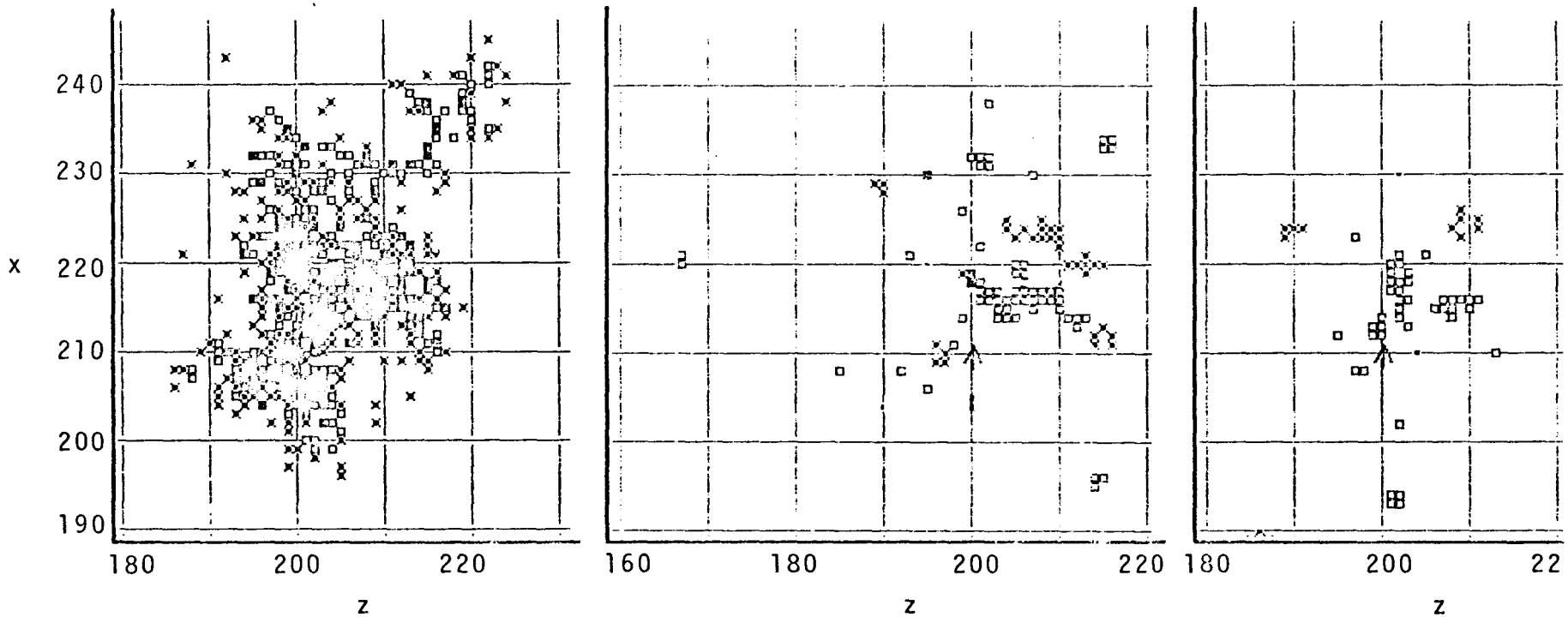

A. PRE-ANNEAL

B. 32 SITE AR

C. 104 SITE AR

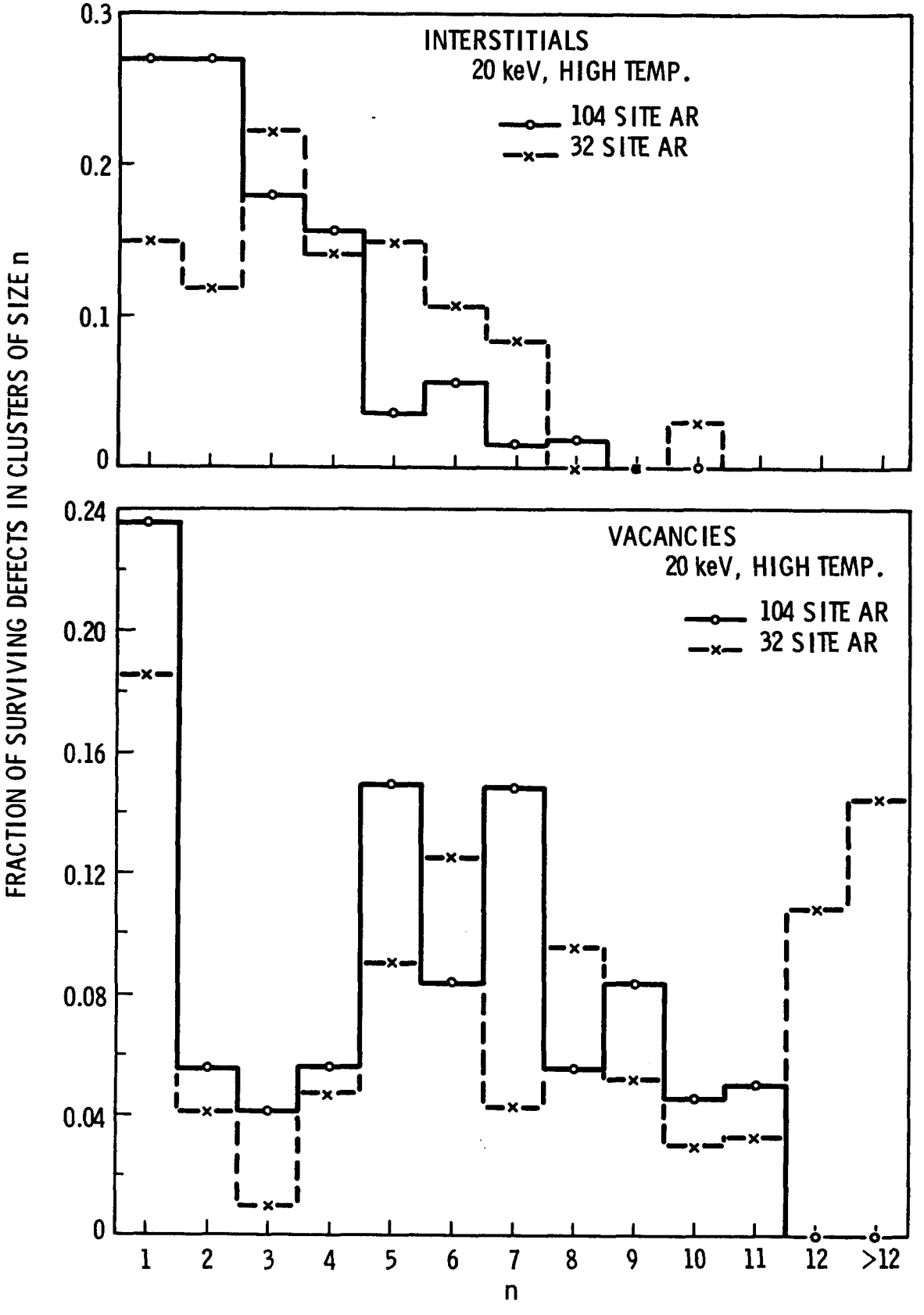
INTERSTITIALS
20 keV, HIGH TEMP.
104 SITE AR
32 SITE AR
VACANCIES
20 keV, HIGH TEMP.
104 SITE AR
32 SITE AR
FRACTION OF SURVIVING DEFECTS IN CLUSTERS OF SIZE n
0.3
0.2
0.1
0
0.24
0.20
0.16
0.12
0.08
0.04
0
1
2
3
4
5
6
7
8
9
10
11
12
>12
n

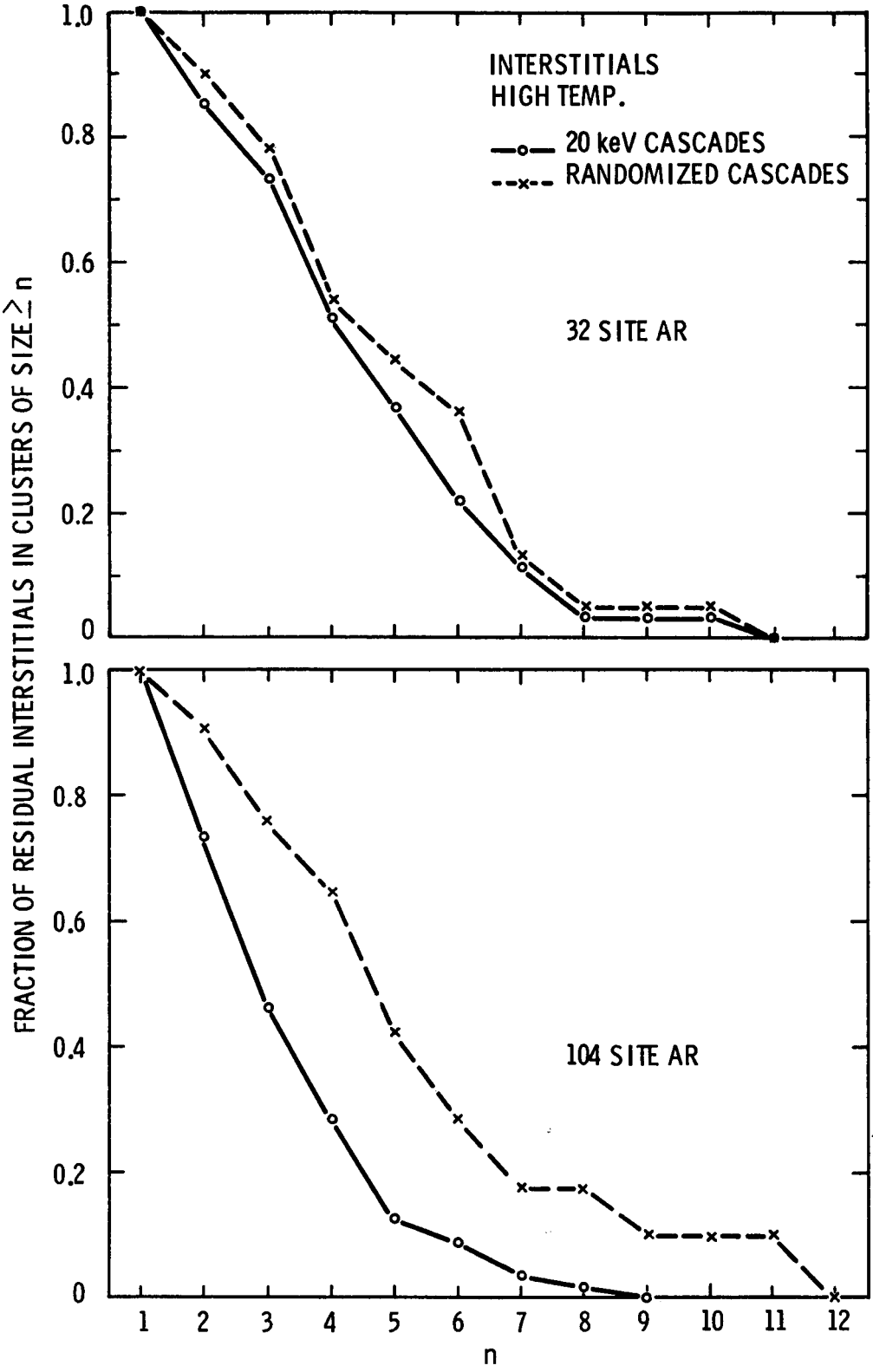
INTERSTITIALS
HIGH TEMP.
20 keV CASCADES
RANDOMIZED CASCADES
32 SITE AR
104 SITE AR
FRACTION OF RESIDUAL INTERSTITIALS IN CLUSTERS OF SIZE ≥ n
n
1.0
0.8
0.6
0.4
0.2
0
1
2
3
4
5
6
7
8
9
10
11
12

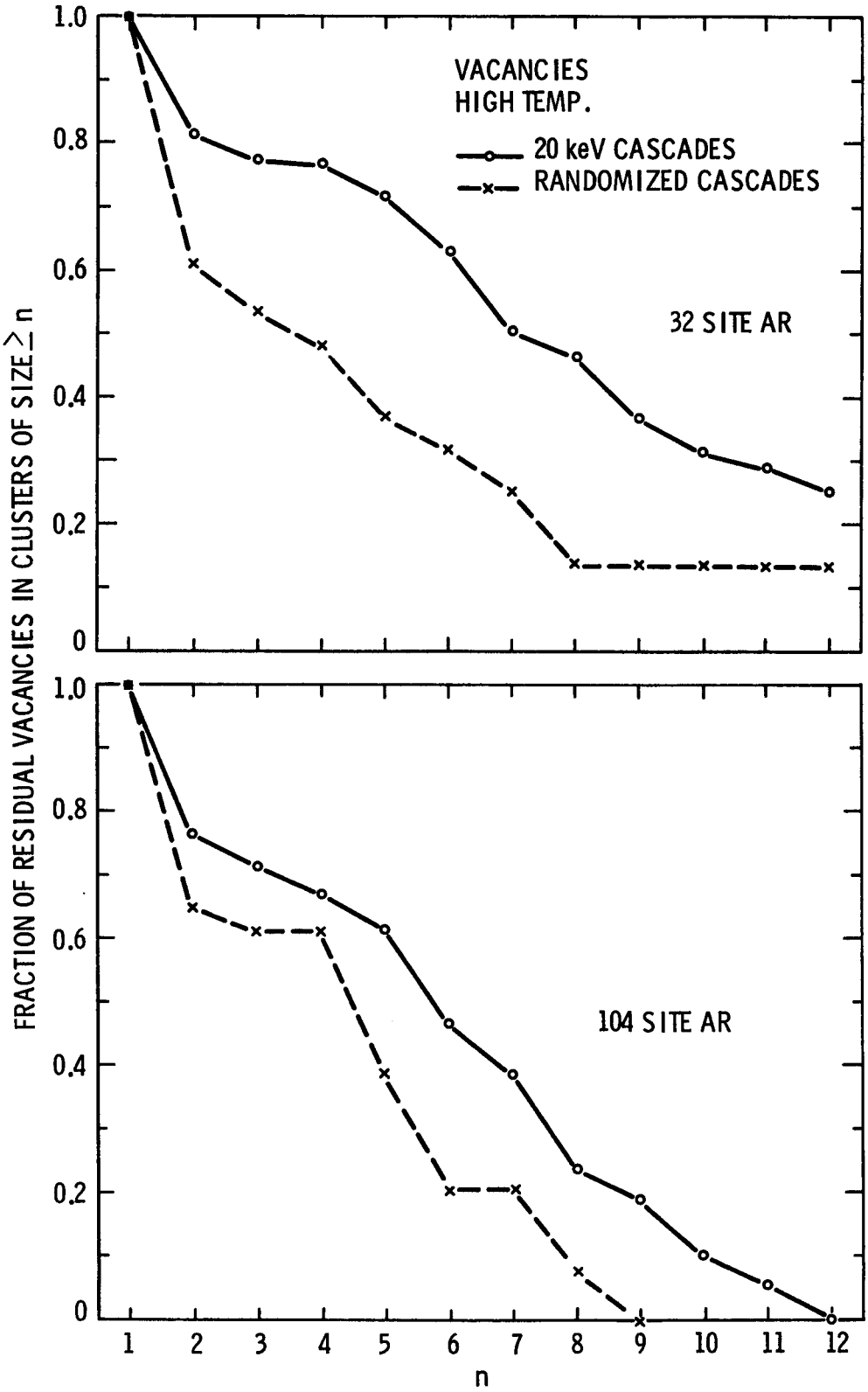
VACANCIES
HIGH TEMP.
20 keV CASCADES
RANDOMIZED CASCADES
32 SITE AR
104 SITE AR
FRACTION OF RESIDUAL VACANCIES IN CLUSTERS OF SIZE ≥ n
n
1.0
0.8
0.6
0.4
0.2
0
1
2
3
4
5
6
7
8
9
10
11
12

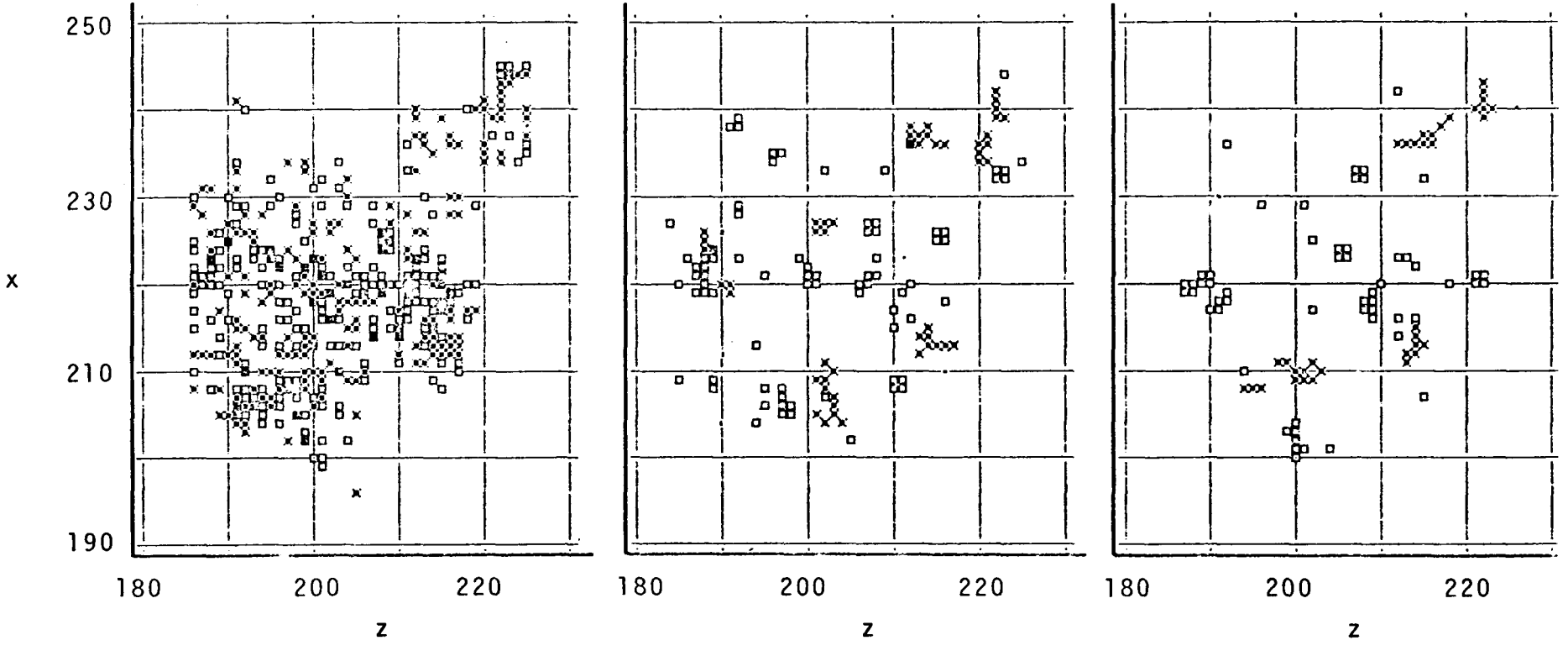

A. PRE-ANNEAL

B. 32 SITE AR

C. 104 SITE AR